

# Fallback accretion in the aftermath of a compact binary merger

Stephan Rosswog,

*School of Engineering and Science, International University Bremen\*, Campus Ring 1, Germany;*

*\* Jacobs University Bremen as of spring 2007*

## ABSTRACT

Recent observations of long and short gamma-ray bursts have revealed a puzzling X-ray activity that in some cases continues for hours after the burst. It is difficult to reconcile such time scales with the viscous time scales that an accretion disk can plausibly provide. Here I discuss the accretion activity expected from the material that is launched into eccentric, but gravitationally bound orbits during a compact binary merger coalescence. From a simple analytical model the time scales and accretion luminosities that result from fallback in the aftermath of a compact binary merger are derived. For the considered mass range, double neutron star binaries are relatively homogeneous in their fallback luminosities. Neutron star black hole systems show a larger spread in their fallback behaviour. While the model is too simple to make predictions about the detailed time structure of the fallback, it makes reasonable predictions about the gross properties of the fallback. About one hour after the coalescence the fallback accretion luminosity can still be as large as  $\sim 10^{45}$  erg/s, a fraction of which will be transformed into X-rays. Large-scale amplitude variations in the X-ray luminosities can plausibly be caused by gravitational fragmentation, which for the high-eccentricity fallback should occur more easily than in an accretion disk.

## 1 INTRODUCTION

Recent observations by Swift and Hete II have confirmed the long-held suspicion that short GRBs have a different central engine than long bursts: they occur at systematically lower redshifts (Fox et al. 2005)<sup>1</sup>, in galaxies with (Hjorth et al. 2005) and without star formation (Berger et al. 2005; Barthelmy et al. 2005), the emitted gamma-ray energy is substantially lower compared to long bursts (Soderberg et al. 2006) and no supernova explosion seems to accompany the burst (Bloom et al. 2006; Hjorth et al. 2005; Fox et al. 2005). These observations are naturally explained by the most popular central engine for short bursts, the coalescence of a compact binary system (Blinnikov et al. 1984; Eichler et al. 1989; Paczyński 1991), but alternative models do exist (e.g. MacFadyen et al. 2005; Levan et al. 2006). The observations, however, have also revealed long-lasting X-ray activity after the main gamma-ray emission phase for about half of the bursts (Burrows et al. 2005; Nousek et al. 2006; O’Brien et al. 2006). Several possible explanations have been suggested (e.g. King et al. 2005; Zhang et al. 2006), among them is the fragmentation of the outer parts of an accretion disk due gravitational instabilities (Perna et al. 2006).

This late-time X-ray flaring is considered a challenge to most models of short GRBs. In this letter, I discuss the X-ray signature from fallback material in the aftermath of a compact binary merger. A fraction of the debris material is launched into eccentric orbits and, at some later time, falls back towards the central remnant. For this material, the time scales are not set by viscous disk time scales, but

instead by the distribution of eccentricities within the fallback material which is a result of the torques that acted during the merger process. This naturally leads to time scales that are orders of magnitudes larger than usual viscous disk time scales.

## 2 A SIMPLE ANALYTICAL MODEL

The question of fallback time scales is addressed by means of a simple analytical model whose initial conditions are taken from a set of recent, three-dimensional smooth particle hydrodynamics (SPH) calculations of the merger of both double neutron stars (DNS) and neutron star black hole (NSBH) systems. The details of the input physics and the numerical techniques are described elsewhere (Rosswog & Davies 2002; Rosswog & Liebendörfer 2003; Rosswog et al. 2003; Price & Rosswog 2006; Rosswog & Price 2006; Rosswog 2006). Here we only summarise the main physical parameters of the calculations, see Tab. 1. A few tens of milliseconds after such a binary encounter the remnant consists of the following parts: a central object (either a neutron star-like object or a black hole), a disk, some material flung into eccentric orbits, but gravitationally bound to the remnant (“fallback material”) and some dynamically ejected debris material. The details of the geometry depend on the type of system (DNS or NSBH) and on the mass ratio. As an example, Fig. 1 shows the matter distribution 22.3 ms after the merger of a 1.1 and 1.6  $M_{\odot}$  DNS system.

Restricted by the Courant-Friedrichs-Lewy time step criterion (typical time steps are of the order  $10^{-7}$  s) the evolution of the merger remnant can never be calculated hydrodynamically up to the interesting time scales of hours. We therefore adopt the following simple analytical model. The SPH-particles that are launched into eccentric orbits, but are still bound to the remnant, are treated as

<sup>1</sup> It has recently been suggested (Berger et al. 2005) that at least 1/4 of the short bursts could lie at redshifts  $z > 0.7$  and would therefore imply substantially larger isotropised energies than was inferred for the first set of detected short GRBs with afterglows.

## 2 Rosswog

**Table 1.** Runs that are used as an input for the analytical model. DNS refers to double neutron star systems, NSBH to neutron star black hole binaries.  $M_1, M_2$  are the masses of the binary components (solar units),  $q$  is the mass ratio, # part. is the total number of SPH particles in the simulation,  $m_{\text{fb},-2}$  is the amount of fallback mass in units of  $10^{-2} M_\odot$  and  $E_{\text{fb}}$  the corresponding energy.

run	type	$M_1, M_2, q$	# part.	$m_{\text{fb},-2}$	$\log(E_{\text{fb}}[\text{erg}])$
DA	DNS	1.4, 1.4, 1.000	2 007 516	3.61	50.9
DB	DNS	1.1, 1.6, 0.733	400 904	3.21	51.0
DC	DNS	1.1, 1.1, 1.000	211 296	3.22	50.8
DD	DNS	1.2, 1.2, 1.000	211 296	2.84	50.7
DE	DNS	1.3, 1.3, 1.000	211 296	3.47	50.8
DF	DNS	1.5, 1.5, 1.000	211 296	3.36	50.9
DG	DNS	1.6, 1.6, 1.000	211 296	3.61	50.9
NA	NSBH	1.4, 4.0, 0.350	600 581	7.40	51.9
NB	NSBH	1.4, 6.0, 0.233	208 165	4.57	51.8
NC	NSBH	1.4, 14.0, 0.100	2 971 627	4.05	51.7
ND	NSBH	1.4, 16.0, 0.088	1 005 401	2.91	51.6
NE	NSBH	1.4, 18.0, 0.078	1 497 453	0.015	49.6

test masses in the gravitational field of the enclosed mass,  $M$ , i.e. it is assumed that hydrodynamic pressure forces can be neglected and the dynamics of each particle can be approximated as a point-mass two-body problem. For each of these particles the angular momentum,  $J_i$ , and their energy,  $E_i$ , can be determined. Together with the particle mass  $m_i \ll M$  these two quantities yield the orbital eccentricity

$$e_i = \sqrt{1 + \frac{2E_i J_i^2}{G^2 m_i^3 M^2}}. \quad (1)$$

The semi-major axis

$$a_i = -\frac{GMm_i}{2E_i} \quad (2)$$

then provides the maximum and the minimum distance of the particle orbit from the origin

$$r_{\text{max},i} = a_i(1 + e_i), \quad r_{\text{min},i} = a_i(1 - e_i). \quad (3)$$

The time until a particle reaches a given radius  $R_{\text{dis}}$  can be calculated by integrating the radial equation

$$\frac{dr}{dt} = \pm \sqrt{\frac{2}{m_i} \left( E_i - V(r) - \frac{J_i^2}{2m_i r^2} \right)}, \quad (4)$$

where  $V$  is the potential energy and the positive (negative) sign refers to the motion away from (towards) the origin. The time that elapses while a particle moves from a radius  $r_1$  to a radius  $r_2$  can be written as

$$\tau_{r_1, r_2} = \pm \int_{r_1}^{r_2} \frac{r dr}{\sqrt{Ar^2 + Br + C}}, \quad (5)$$

where the constants  $A = \frac{2E_i}{m_i}$ ,  $B = 2GM$  and  $C = -\frac{J_i^2}{m_i^2}$  have been introduced. The integral appearing in eq. (5) can be solved analytically

$$I_{r_1, r_2} = \left[ \frac{\sqrt{Ar^2 + Br + C}}{A} + \frac{B}{2A\sqrt{-A}} \arcsin \left( \frac{2Ar + B}{\sqrt{-D}} \right) \right]_{r_1}^{r_2}, \quad (6)$$

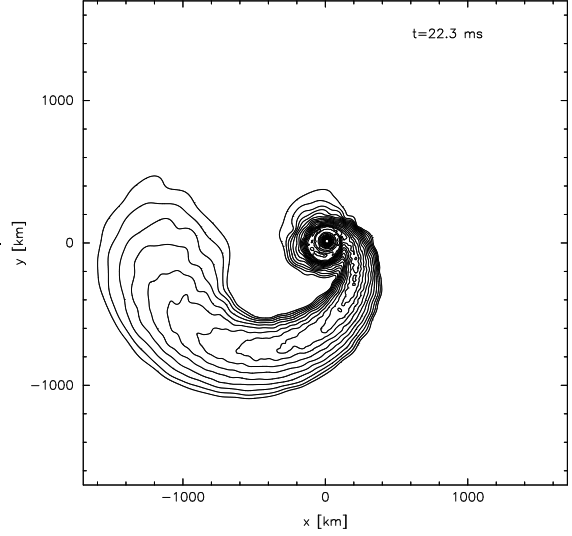


**Figure 1.** Contours of the mass density ( $10^7 - 10^{14} \text{ g cm}^{-3}$ ) 22.3 ms after the merger of a double neutron star system with 1.1 and 1.6  $M_\odot$ . In this case, about  $0.03 M_\odot$  are launched into eccentric orbits and will finally fall back towards the centre.

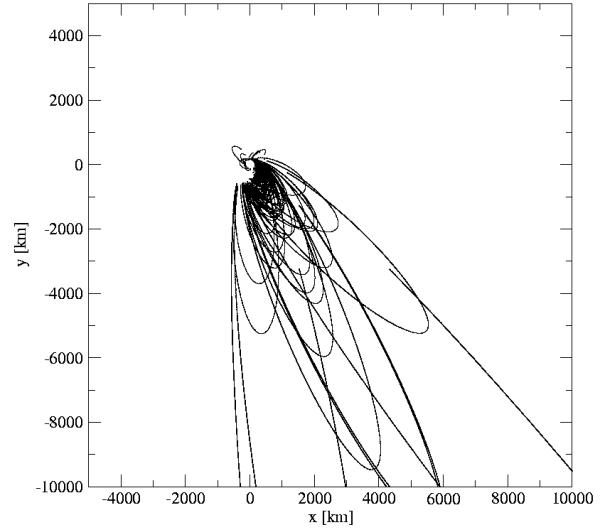


**Figure 2.** A sample of fallback trajectories resulting from a double neutron star merger with 1.1 and 1.6  $M_\odot$ . The dissipation radius,  $R_{\text{dis}}$  in this case was 100 km.

where  $D = 4AC - B^2$ . The time that elapses from a particle's present radius,  $r_i$ , until its energy is dissipated at a radius  $R_{\text{dis}}$  is then given by the contributions with the appropriate signs:

$$\tau_i = \begin{cases} I_{r_i, r_{\text{max},i}} + I_{r_{\text{max},i}, R_{\text{dis}}} & \text{for } \vec{v}_i \cdot \vec{r}_i > 0 \\ I_{r_i, R_{\text{dis}}} & \text{for } \vec{v}_i \cdot \vec{r}_i < 0 \end{cases}. \quad (7)$$

For the radius, where the fallback energy is dissipated,  $R_{\text{dis}}$ , we take in the double neutron star case the disk radius at the end of the numerical simulation. This is conservative in the sense that the disk will shrink, see below, and therefore the assumption of a radius fixed at  $R_{\text{dis}}$  yields shorter timescales and lower accretion luminosities. For the black hole cases, I choose  $R_{\text{dis}} = 10GM/c^2$ , so just outside the innermost stable circular orbit of a non-rotating

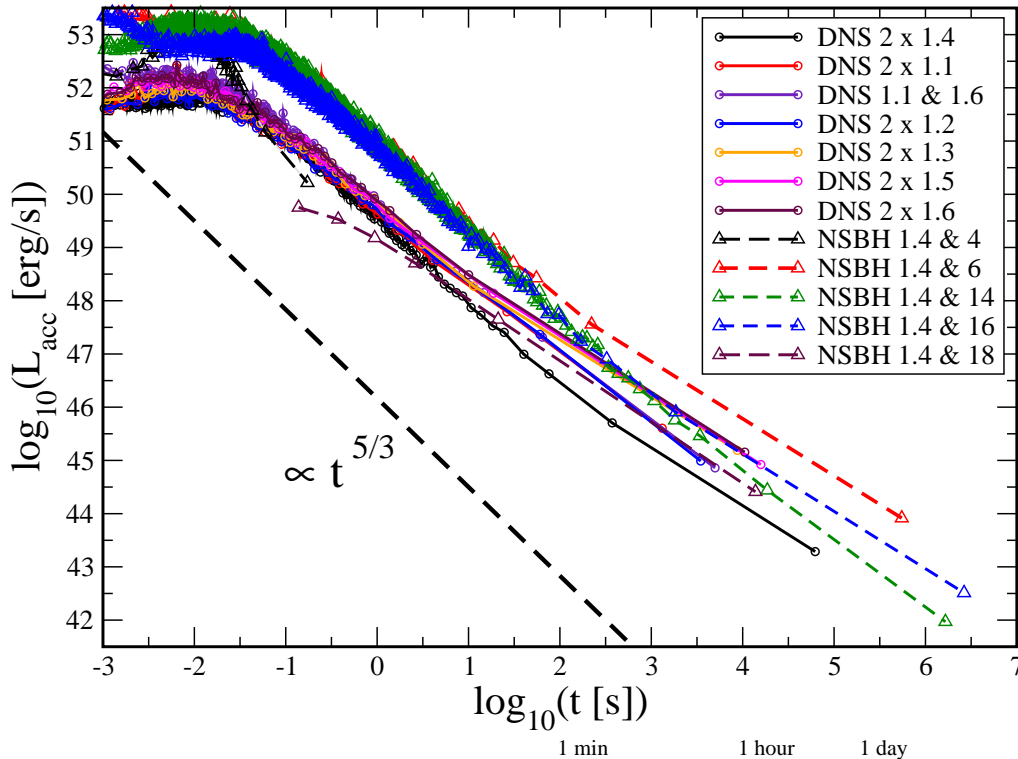


**Figure 3.** Fallback accretion luminosity for various compact binaries. Circles refer to double neutron star systems (DNS), triangles to neutron star black hole mergers (NSBH). Note that the rightmost point is determined by the mass resolution of the simulation. For reference a straight line with slope 5/3 is shown.

(Schwarzschild-) black hole at  $R_{\text{ISCO}} = 6GM/c^2$ . The details of the fallback times and energies change slightly with  $R_{\text{dis}}$ , but none of the conclusions of this paper depends on the exact numerical value of  $R_{\text{dis}}$ .

As an illustration, I show in Fig. 2 a set of fallback trajectories. The initial conditions were taken from the double neutron star merger calculation with 1.1 and 1.6  $M_{\odot}$  that is shown in Fig. 2. 200 randomly chosen trajectories out of the more than 5800 fallback particles are plotted. There is a broad distribution of eccentricities and fallback times, while some particles return from their initial position directly towards the central object, others follow highly eccentric orbits out to distances of many 10 000 km before they come to a halt and fall back towards the centre.

### 3 FALLBACK ACCRETION

Fig. 3 shows the accretion luminosities,  $L_{\text{acc}} = dE_{\text{fb}}/dt$ , derived for the various DNS and NSBH systems. Here,  $E_{\text{fb}}$  denotes the difference between the potential plus kinetic energy at the start radius,  $r_i$ , and the potential energy at the dissipation radius,  $R_{\text{dis}}$ . The curves have been obtained by binning the energies contained in the fallback material,  $E_{\text{fb}}$ , according to the corresponding fallback times,  $\tau_i$ , see eq. (7). A fraction  $\epsilon_X$  of this energy is channelled

into X-rays,  $L_X = \epsilon_X L_{\text{acc}}$ .

The double neutron star cases form a rather homogeneous class with respect to their fallback accretion, in all cases the fallback material is approximately 0.03  $M_{\odot}$ , see Tab. 1. After an initial, short-lived plateau, the luminosity falls off with time close to the expected 5/3-power law (Rees 1988; Phinney 1989). It has to be pointed out that the last point in these curves is determined by the numerical mass resolution in the hydrodynamics simulations and should therefore be interpreted with some caution. All other points should be a fair representation of the overall fallback activity. Typically, the X-ray luminosity about one hour after the coalescence is  $L_X \sim \left(\frac{\epsilon_X}{0.1}\right) \cdot 10^{44}$  erg/s. For the investigated mass range, the spread in the luminosities one hour after the coalescence is about one order of magnitude.

The neutron star black hole cases show a larger diversity. The mass in the fallback material of different mass ratios varies by about a factor of 500, see Tab. 1, an hour after the merger the accretion luminosities of the different NSBH systems differ by about two orders of magnitude. Also the involved time scales change strongly with the binary mass ratio. For example, the 1.4 and 4  $M_{\odot}$  NSBH case does not produce much eccentric fallback material. Accretion, at least to the resolvable level, is over in  $\sim 0.2$  s. This accretion period may produce a short GRB, but probably not much X-ray activity. The 1.4 and 18  $M_{\odot}$  NSBH system is at the other extreme: its

peak luminosity is lower by three orders of magnitude but extends (at a resolvable level) up to about one hour. The mass ratios in between could possibly produce a (weak) GRB and extended X-ray activity up to about one day after the burst.

#### 4 SUMMARY

A simple analytical model was presented and used to derive the fallback time scales and accretion luminosities in the aftermath of a compact binary merger. The initial conditions are taken from a large set of 3D hydrodynamical simulations. The main assumption of this model is that the fallback material is ballistic, i.e. that hydrodynamical pressure forces can be neglected. This is a good approximation for the largest part of the time spent along the individual trajectories, therefore, the fallback time scales can be considered valid estimates. The assumption may only break down when the vicinity of remnant is approached, but this will only cause minor corrections to the fallback time scale and luminosity estimates.

For the range of mass ratios (1.1 to 1.6  $M_{\odot}$ ) that I have considered, double neutron star systems show a rather homogeneous fallback behaviour. At one hour after the coalescence their X-ray luminosity is still  $\sim 10^{44} (\epsilon_X/0.1)$  erg/s. Neutron star black hole mergers provide a larger spread in their fallback behaviour. An hour after the tidal disruption of the neutron star, their range in fallback luminosities is about two orders of magnitudes. Some mass ratios could produce a GRB, but not much X-ray activity, others may produce X-ray flaring only but no GRB, and yet other systems can produce both.

Since this simple approach does not account for self-gravity and gas pressures, it tends to produce too smooth results. The shown luminosity curves should therefore be interpreted as temporal averages. The original accretion disks, such as the one seen in Fig. 1 extending out to  $\sim 200$  km, are consumed on a viscous time scale of

$$\tau_{\text{visc}} \sim 1/\alpha\Omega_K \sim 0.05\text{s} \left(\frac{R}{200\text{ km}}\right)^{3/2} \left(\frac{0.1}{\alpha}\right) \left(\frac{2.5M_{\odot}}{M_{\text{c.o.}}}\right), \quad (8)$$

where  $\alpha$  is the Shakura-Sunyaev viscosity parameter (Shakura & Sunyaev 1973),  $R$  the disk radius,  $\Omega_K$  the Kepler frequency and  $M_{\text{c.o.}}$  is the mass of the central object. The outer parts of this disk are constantly fed by material that continuously falls back so that a low mass remnant disk is maintained until late times. The observed X-ray activity is expected to be produced by this disk and its interaction with the high-eccentricity fallback material.

Large-scale amplitude variations in the lightcurves (“flares”) can occur if the fallback material becomes subject to self-gravitational instabilities. Whether a lump of gas is prone to this instability depends on the ratio of the cooling time,  $\tau_{\text{cool}}$ , and the local dynamical time,  $\tau_{\text{dyn}}$ . Gammie (2001) finds for the case of thin accretion disks the condition  $\tau_{\text{cool}} \leq 3\tau_{\text{dyn}}$ . Gravitational fragmentation is common in the outer regions of the accretion disks of AGNs (Shlosman et al. 1990) and of young stellar objects (Adams & Lin 1993). Perna et al. (2006) have suggested that such a fragmentation in the outskirts of an accretion disk could be the common mechanism behind the flaring observed in both long and short bursts. They note, however, that it may be difficult to reach the suitable conditions in the case of a compact binary merger. The fragmentation idea has recently been examined in more detail by Piro and Pfahl (2006) for the case of collapsar disks. They argue that fragmentation may occur near the radius where

alpha-particles are photodissociated since this consumes about 7 MeV of thermal energy per nucleon and thus provides an efficient cooling mechanism. They suggest that even neutron star-like objects of low masses may form, but conclude that their disruption would be too rapid to account for the observed, post-GRB X-ray flaring.

Some the eccentric fallback material could undergo gravitational fragmentation into one or several bound objects. Since there is a large spread in orbital eccentricities, it seems unlikely that a large fraction of the fallback material agglomerates into a single fragment. If fragmentation occurs, it will do so only locally and for a small fraction of the material. A fragment of mass  $m_f$  will release a flare energy of  $E_f \sim 10^{49} \text{erg} \left(\frac{\epsilon_X}{0.1}\right) \left(\frac{M_{\text{c.o.}}}{3 M_{\odot}}\right) \left(\frac{m_f}{0.003 M_{\odot}}\right) \left(\frac{200 \text{ km}}{R_{\text{dis}}}\right)$ . When such a fragment of radius  $R_f$  falls back towards the centre, it becomes tidally disrupted at a distance  $R_{\text{tid}} = (M_{\text{c.o.}}/m_f)^{1/3} \cdot R_f$ , or, if the remnant disk radius is larger than  $R_{\text{tid}}$ , the fragment will impact with nearly free-fall velocity on that disk. In both cases, it will trigger violent X-ray flaring activity.

In this picture the GRB is produced by the massive accretion disk that can form early on in the merger. The GRB duration is determined by the viscous time scale on which this disk is consumed. The late-time X-ray activity, in contrast, is caused by the fallback of a smaller amount, about a tenth of the disk mass, of high-eccentricity material which is a natural outcome of the merger. The fallback time scales are set by the distribution of eccentricities in this material, which is a result of the torques that acted during the merger process.

#### ACKNOWLEDGEMENTS

The calculations in this paper have partly been performed on the JUMP computer of Forschungszentrum Jülich.

#### REFERENCES

- Adams F. C., Lin D. N. C., 1993, in *Protostars and Planets III*, Levy E. H., Lunine J. I., eds., pp. 721–748
- Barthelmy S. D., et al., 2005, *Nature*, 438, 994
- Berger E. et al., 2005, *Nature*, 438, 988
- Berger E. et al., 2006, submitted to *ApJ*, astro-ph/0611128
- Blinnikov S. I., et al., 1984, *Soviet Astron. Lett.*, 10, L77
- Bloom J. S. et al., 2006, *ApJ*, 638, 354
- Burrows D. N. et al., 2005, *Science*, 309, 1833
- Eichler D., Livio M., Piran T., Schramm D. N., 1989, *Nature*, 340, 126
- Fox D. B. et al., 2005, *Nature*, 437, 845
- Gammie C. F., 2001, *ApJ*, 553, 174
- Hjorth J. et al., 2005, *Nature*, 437, 859
- Levan, A.J. et al., astro-ph/0601332 (2006)
- MacFadyen A. I., Ramirez-Ruiz E., Zhang W., 2005, astro-ph/0510192
- Nousek J. A. et al., 2006, *ApJ*, 642, 389
- O’Brien P. T. et al., 2006, *ApJ*, 647, 1213
- Paczyński B., 1991, *Acta Astron.*, 41, 257
- Perna R., Armitage P. J., Zhang B., 2006, *ApJL*, 636, L29
- Piro A., Pfahl, E., 2006, submitted to *ApJL*, astro-ph/0610696
- Phinney E. S., 1989, in *IAU Symp. 136: The Center of the Galaxy*, Morris M., ed., pp. 543
- Price D., Rosswog S., 2006, *Science*, 312, 719

- King, A.R. et al., 2005, ApJ 630, L113  
Rees M. J., 1988, Nature, 333, 523  
Rosswog S., Revista Mexicana de Astronomia y Astrofisica, 2006,  
in press  
Rosswog S., Davies M. B., 2002, MNRAS, 334, 481  
Rosswog S., Liebendörfer M., 2003, MNRAS, 342, 673  
Rosswog S., Price D., 2006, in prep.  
Rosswog S., Ramirez-Ruiz E., Davies M. B., 2003, MNRAS, 345,  
1077  
Shakura N. I., Sunyaev R. A., 1973, A & A, 24, 337  
Shlosman I., Begelman M. C., Frank J., 1990, Nature, 345, 679  
Soderberg A. M. et al., 2006, ApJ, 650, 261  
Zhang B. et al., 2006, ApJ, 642, 354